Electronic structure of Ag_2O

L. H. Tjeng, M. B. J. Meinders, J. van Elp, J. Ghijsen,* and G. A. Sawatzky
Department of Solid State and Applied Physics, Material Science Centre, University of Groningen, Nijenborgh 18, NL-9747 AG Groningen, The Netherlands

R. L. Johnson†
Max-Planck Institute for Solid State Physics, Heisenbergstrasse 1, D-7000 Stuttgart 80, Federal Republic of Germany
(Received 15 June 1989)

The electronic structure of Ag_2O has been investigated by photoelectron, Auger-electron, and bremsstrahlung isochromat spectroscopy. The experimental results are compared with model one-particle band-structure and two-particle cluster calculations. We extract values for the on-site Ag $4d$ and O $2p$ energies, the Ag $4d$–O $2p$ transfer integrals, as well as the on-site Coulomb Ag $4d$-$4d$ and O $2p$-$2p$ interactions. A comparison with Cu_2O and CuO is made, and the differences are discussed in view of high-T_c superconductivity and the instability of AgO.

I. INTRODUCTION

It is generally believed that the CuO_2 planes in oxide superconductors are of crucial importance for high superconducting transition temperatures. For this reason and because of similar Cu-O distances, Cu_2O and CuO are often used as model compounds for a detailed study of the electronic structure.[1,2] Because of the similarities between Ag and Cu, it is interesting to try to understand why oxidic Ag compounds are not high-T_c superconductors. The differences in the electronic structure of Ag and Cu oxides could provide more insight into those characteristics that are of importance for high-T_c superconductivity. Ag_2O has the same crystallographic structure as Cu_2O (Table I, Ref. 3), and one might expect a similar electronic structure. On the other hand AgO is less stable than CuO and has a quite different crystal structure.[4–6] One might ask if this can be understood in terms of the differences in the one electron energies and Coulomb and exchange interactions.

A better understanding of the electronic structure of Ag_2O is also required to test the existence of various binding types of adsorbed oxygen on Ag metal surfaces.[7–9] Ag_2O is a model compound for the study of (photo) electrochemical[10,11] and catalytic processes, such as the epoxidation of ethylene.[12,13]

Although several x-ray photoemission spectroscopy (XPS) (Refs. 14–18) and Auger-electron spectroscopy (Refs. 17–19) studies have been carried out on Ag_2O, no published work on (photon-energy-dependent) ultraviolet photoemission spectroscopy (UPS), bremsstrahlung isochromat spectroscopy (BIS), or comparison of the spectra to electronic-structure calculations exist.[20] Moreover, the spectra presented so far are based on ill-defined Ag_2O powder samples, showing double O 1s and/or C 1s core-level peaks.

TABLE I. Crystallographic parameters of Ag_2O and Cu_2O (from Ref. 3). The unit cell contains six atoms. The oxygen atoms form a bcc lattice and are tetrahedrally coordinated by noble-metal atoms, while the noble-metal atoms are linearly coordinated by the oxygen atoms.

	Ag_2O (Å)	Cu_2O (Å)
Lattice parameter (cubic)	$a=4.74$	$a=4.27$
Shortest distances	$d_{Ag\text{-}O}=2.05$	$d_{Cu\text{-}O}=1.84$
	$d_{Ag\text{-}Ag}=3.34$	$d_{Cu\text{-}Cu}=3.02$
	$d_{O\text{-}O}=4.10$	$d_{O\text{-}O}=3.68$

II. EXPERIMENTAL SETUP AND SAMPLE PREPARATION

XPS and BIS measurements were performed using a modified Kratos 200 spectrometer. The XPS source was the unmonochromatized Al $K\alpha$ line (1486.6 eV), which corresponds also to the energy of the photons collected by BIS. The instrumental broadening is estimated to be 1.0 eV for XPS and 0.7 eV for BIS. UPS data were collected using an ADES 400 spectrometer. The resolution was 0.1 eV for He I and 0.25 eV for He II. Photon-energy-dependent UPS measurements were carried out at the FLIPPER–II beamline at Hamburger Synchrotronstrahlungslabor in Hamburg. The synchrotron radiation photon energy ranges from 16 to 140 eV, and the overall resolution varies between 0.15 to 0.5 eV accordingly. The base pressure of all three spectrometers is in the low 10^{-10} Torr range.

The sample was prepared starting with 99.999% pure silver. The metal surface was mirror polished before introduction into the spectrometer. In a first step, silver was Ar sputter cleaned until a clean XPS spectrum was obtained. Thereafter, the valence-band spectrum was recorded to determine the position of the Fermi level which was subsequently used as the reference of binding and kinetic energies. In the preparation chamber of each of the above-mentioned spectrometers, with a base pressure in the low 10^{-9} Torr range, Ag_2O was made by ex-

posing the clean silver metal at room temperature to a (cold-discharge–magnetically confined) free radical oxygen source, operating at a total oxygen pressure of 8×10^{-5} Torr. After 1.5 h the color of the sample was yellowish to brownish, indicating that a Ag_2O layer with several hundreds of Å had formed. The layer was thick enough to conceal the underlying metal, but thin enough to allow good compensation of any charging effect from XPS, UPS, and BIS.

The Ag_2O sample remained stable in the ultra-high-vacuum conditions for at least 8 h under XPS and UPS light sources. The electron beam used in BIS, however, induced detectable decomposition after 1 h of measurement. Therefore, repeated cycles of Ar sputter cleaning and oxidation followed by 30 min of BIS measurements were made in order to collect enough photons.

III. MODEL CALCULATIONS

The objective of the model calculations is to obtain the one-hole and two-hole density of states (DOS) of the valence band, to be compared with valence-band photoemission and Auger spectra, respectively. The model Hamiltonian is given by

$$H=H_0+H_1 ,$$

$$H_0=\sum_{i,m}\varepsilon_d d^\dagger_{im}d_{im}+\sum_{j,n}\varepsilon_p p^\dagger_{jn}p_{jn} + \sum_{i,j,m,n}T_{pd}(i,j;m,n)(d^\dagger_{im}p_{jn}+p^\dagger_{jn}d_{im}) ,$$

$$H_1=\sum_{i,m,m',m'',m'''}U_{dd}(m,m',m'',m''') \times d^\dagger_{im}d_{im'}d^\dagger_{im''}d_{im'''} + \sum_{j,n,n',n'',n'''}U_{pp}(n,n',n'',n''') \times p^\dagger_{jn}p_{jn'}p^\dagger_{jn''}p_{jn'''} .$$

Here H_0 describes one-particle and H_1 two-particle interactions. The operators $d^\dagger$ and $p^\dagger$ create Ag $4d$ and O $2p$ holes with on-site energy ε_d and ε_p, respectively. The indices i and j label the sites, and $m,m',m'',m''',n,n',n'',n'''$ denote orbital and spin quantum numbers. T_{pd} is the O $2p$–Ag $4d$ transfer integral, which is restricted here to nearest neighbors only and which is expressed in terms of Slater-Koster two-center integrals $(pd\sigma)$ and $(pd\pi)$.[21] U_{dd} and U_{pp} are the respective on-site Ag $4d$-$4d$ and O $2p$-$2p$ Coulomb and exchange energies. Using the full atomic multiplet theory, U_{dd} is expressed in terms of the Racah A, B, and C parameters, and U_{pp} in terms of Slater F^0 and F^2 integrals.[22,23] In this Hamiltonian we have neglected all the core levels and even more important the Ag $5s,5p$ as well the empty O bands. These are quite high in energy and therefore we assume that their influence via hybridization etc., can be treated as a renormalization of the effective model parameters. We do not take into account the next-nearest-neighbor transfer integrals, since the next-nearest-neighbor distances are at least 60% larger than the nearest-neighbor distances (Table I), which according to Harrison's relationships[24] can be estimated to give integrals by an order of magnitude smaller. We have also neglected spin-orbit splitting for Ag, which is about 0.5 eV, and the interatomic O $2p$–Ag $4d$ Coulomb interaction U_{pd}, which is expected to be smaller than 1 eV by comparison to Cu_2O (Ref. 2).

It has been shown by Ghijsen *et al.*[1] that Cu_2O is an essentially closed-shell system. It is therefore expected, and will be justified by experimental data, that the ground state of Ag_2O is given by a closed Ag $4d$ and O $2p$ shell configuration. This means that in valence-band photoemission, a one-hole problem, described by H_0, has to be solved. The diagonalization of H_0 can be done in an exact way for i and j covering the whole lattice, using the Slater-Koster linear combination of atomic orbitals (LCAO) tight-binding (TB) method,[21] to obtain the total and Ag $4d$ partial DOS. In studying the Ag $M_5N_{45}N_{45}$ and O $KL_{23}L_{23}$ Auger-electron spectra, a two-hole problem, described by H_0+H_1, has to be solved. Here we restrict ourselves to a $(Ag_7O_2)^{3+}$ cluster with a Ag atom in the center when studying the Ag $M_5N_{45}N_{45}$ Auger line, and to a $(Ag_4O_5)^{6-}$ cluster with an O atom in the center when analyzing the O $KL_{23}L_{23}$ Auger line. In this way we obtain the Ag $4d^8$ and O $2p^4$ projected DOS at the respective central atoms.

IV. RESULTS

A. Core levels

We first consider the core-level spectra of oxygen and silver, and use them to check the composition of our material. Their energies are listed in Table II, which also includes data from clean Ag metal for reference purposes.

TABLE II. Core-level binding energies and Auger kinetic energies (eV) of Ag_2O and Ag, referenced to the Fermi level inside the solid.

		Ag_2O	Ag
Ag $3d_{5/2}$	(binding energy)	367.6±0.2	368.0±0.2
Ag $3d_{3/2}$		373.6±0.2	374.0±0.2
O $1s$		528.9±0.2	
Ag $M_5N_{45}N_{45}$	(kinetic energy)	351.9±0.3	352.5±0.3
Ag $M_4N_{45}N_{45}$		357.3±0.3	358.5±0.3
O $KL_{23}L_{23}$		513.9±0.3	

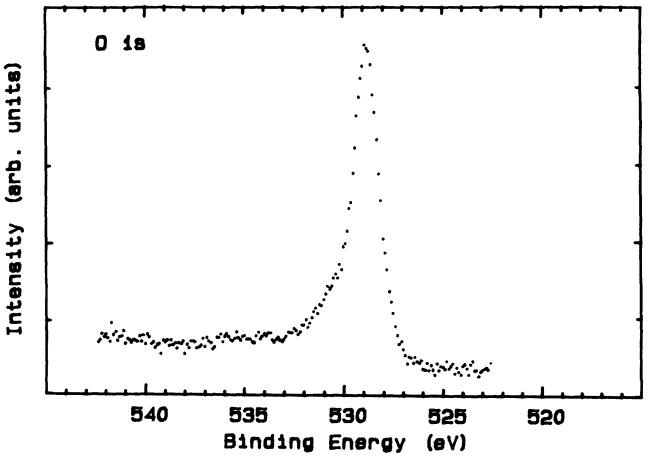

FIG. 1. O 1*s* XPS from Ag_2O.

The O 1*s* spectrum is shown in Fig. 1. It consists of a single narrow peak, 1.2 eV full width at half maximum (FWHM). Therefore, and also because no C 1*s* peak could be detected, we are confident, that our sample is free from species such as water, hydroxides, carbonates, and adsorbed oxygen, in contrast to reports in the literature,[14–19] where a second broad peak (3 eV FWHM) at several eV higher binding energies is present in the O 1*s* spectra, and where some C 1*s* peaks can also be seen. This is not surprising since published results were obtained from Ag_2O powders, which had been exposed to air.

The Ag $3d_{5/2}$ and $3d_{3/2}$ spectra are displayed in Fig. 2. The absence of any satellite structure herein, as well as in the O 1*s* spectrum, is consistent with the expectation that no AgO has been formed. It is very unlikely that AgO is stable under ultra-high-vacuum conditions because the oxygen dissociation pressure is orders of magnitude larger than that of Ag_2O, which itself is already high:

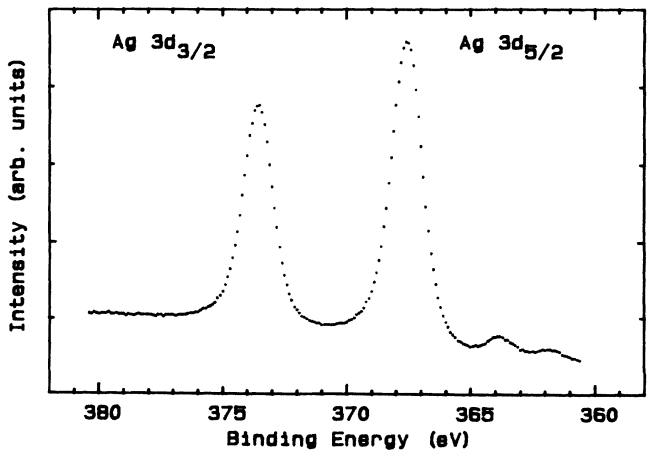

FIG. 2. Ag $3d_{5/2}$ and $3d_{3/2}$ XPS from Ag_2O.

5×10^{-4} atm at room temperature and 1 atm at 100 °C,[25,26] in thermodynamic equilibrium.

Using above-mentioned spectra, together with known photoionization cross sections[27] and mean free paths,[28]

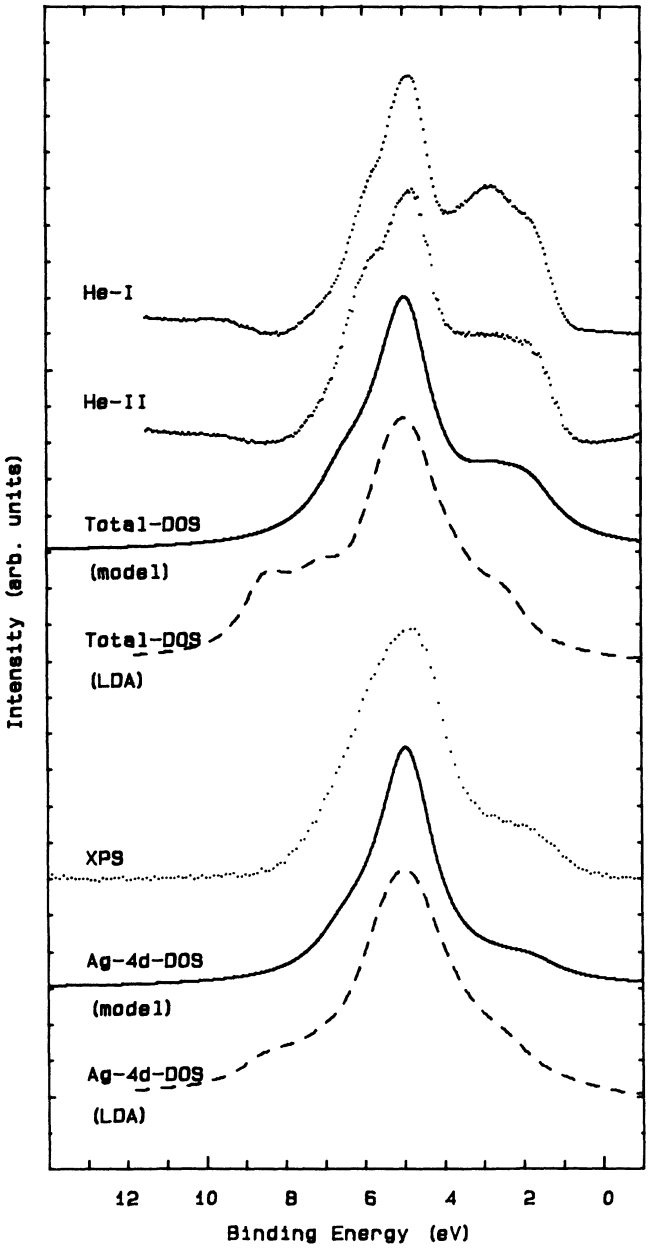

FIG. 3. Valence-band UPS, XPS, and DOS from Ag_2O, normalized to the peak height. The dotted lines show the experimental spectra using He I (21.2 eV), He II (40.8 eV), and Al $K\alpha$ (1486.6 eV, XPS) sources, corrected for analyzer transmission and electron scattering. The solid and dashed curves are the calculated DOS's obtained from the model Slater-Koster LCAO-TB and the LDA band-structure [Czyzyk *et al.* (Ref. 20)] methods, respectively. The theoretical curves have been shifted to align the main peak. The Lorentzian broadening is 1.2 eV for the total DOS and 1.6 eV for the Ag 4*d* DOS.

the oxygen-silver concentration ratio has been verified and found to be the same as the oxygen-copper concentration ratio in Cu_2O.

B. Valence band

Valence-band spectra measured at various photon energies are displayed in Figs. 3 and 4. Utilizing the known energy dependence of the photoionization cross section we can identify regions of primarily O $2p$ or Ag $4d$ spectral weight. The atomic cross-section ratios, weighted by the number of electrons per atom, are $\sigma(O\ 2p)/\sigma(\mathrm{Ag}\ 4d)\approx 1.0$, 0.3, and 0.2 for $h\nu=21.2$ (He I), 40.8 (He II), and 1486.6 (Al -$K\alpha$) eV, respectively.[27] This ratio is approximately 3.1 for $h\nu\approx 130$ eV, at which energy the Ag Cooper-minimum occurs. Therefore, in XPS we see primarily the Ag $4d$ spectral weight (Fig. 3), which in Ag_2O is concentrated around 5 eV, whereas at the Cooper minimum we see the O $2p$ spectral weight (Fig. 4), which is concentrated at 2–4 eV. At this phonon energy the O $2s$ peak can also be clearly seen, located at 21.2 eV binding energy. In Fig. 3, the calculated Ag $4d$ one-hole DOS is compared with the XPS, and the calculated total one-hole DOS with the He I and He II UPS, where the O $2p$ and Ag $4d$ cross sections are comparable. A good resemblance between the one-particle theory and experiment

TABLE III. Parameter values (eV) used in the model Hamiltonian describing the electronic structure of Ag_2O and Cu_2O (Ref. 2).

			Ag_2O	Cu_2O
One-particle parameters	ε_d		4.9±0.2	3.1±0.2
	ε_p		3.4±0.2	5.6±0.2
	T_{pd}	$(pd\sigma)$	1.3±0.2	1.7±0.2
		$(pd\pi)$	0.6±0.1	0.7±0.1
Two-particle parameters	U_{dd}	A	4.4±0.5	7.4±0.5
		B	0.09	0.15
		C	0.54	0.58
	U_{pp}	F^0	6.8±0.5	5.5±0.5
		F^2	6.0	6.0

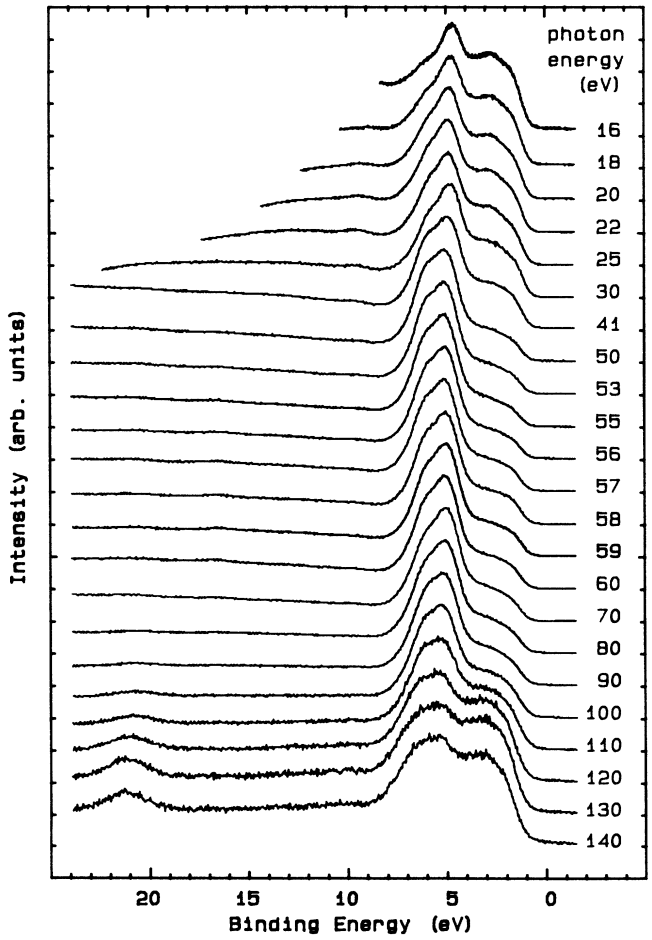

FIG. 4. Valence-band UPS from Ag_2O, using various photon energies, normalized to the peak height and corrected for analyzer transmission. The Ag $4d$ Cooper minimum is at 130 eV.

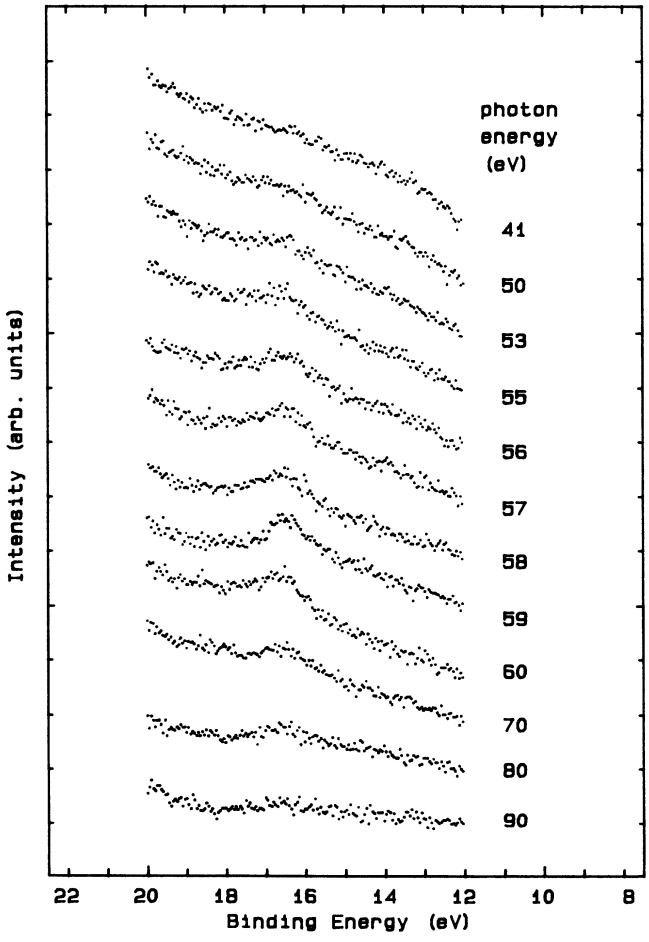

FIG. 5. Resonance photoemission at the Ag $4p$ edge (56 eV). The spectra are normalized to the main peak at 5 eV binding energy and corrected for analyzer transmission.

has been obtained using parameter values as listed in Table III, which also displays the values obtained for Cu_2O (Ref. 2).

A closer look at the valence-band spectra shown in Fig. 5 reveals that a weak resonance is observed at 16.5 eV binding energy, when scanning the photon energy through the Ag 4*p* edge ($h\nu \approx 56$ eV).

It is interesting to note that the valence-band spectra reveal no structure at binding energies between 8 and 12 eV. This means that the pronounced dispersionless structures at 8.9 and 9.7 eV as observed in angle-resolved ultraviolet photoemission from the so-called "weakly" and, respectively, "strongly" bound oxygen on Ag(111) and Ag(110) surfaces,[8,9] are probably not originating from a strong hybridization of the O 2*p* with the Ag 4*d* orbitals alone.

C. Conduction band and band gap

The BIS result on Ag_2O is displayed in Fig. 6, along with the XPS spectrum. The energy in both BIS and XPS is referred to the Fermi level, measured prior to oxidation. The bottom of the conduction band is located at 0.3 eV and the top of the valence band at -1.0 eV, resulting in a band gap of 1.3 eV, in good agreement with a previous photoconductive determination.[29,30] For comparison, the BIS and XPS spectra for Cu_2O are also displayed in Fig. 6. Table IV lists the valence- and conduction-band edge positions and band gap values of Ag_2O and Cu_2O.

D. Auger lines

The O $KL_{23}L_{23}$, Ag $M_5N_{45}N_{45}$, and Ag $M_4N_{45}N_{45}$ Auger spectra are shown in Figs. 7 and 8, and the peak positions are listed in Table II, together with data for the clean Ag metal for reference purposes. In Figs. 7 and 8,

TABLE IV. Position of valence- and conduction-band edges with respect to the Fermi level, magnitude of the band gap, and *d*-(*sp*) charge-transfer energy (Δ_{dsp}) in Ag_2O and Cu_2O (eV). Δ_{dsp} is the energy distance between the *d* on-site energy (ε_d) and the bottom of the (*sp*) conduction band.

	Ag_2O	Cu_2O
Top of the valence band	-1.0 ± 0.1	-0.6 ± 0.1
Bottom of the conduction band	0.3 ± 0.2	1.6 ± 0.2
Band gap	1.3 ± 0.3	2.2 ± 0.3
d-(*sp*) charge-transfer energy (Δ_{dsp})	5.2 ± 0.4	4.7 ± 0.4

the kinetic energy scale has been translated into a two-hole binding energy scale by subtracting the O 1*s* and Ag $3d_{5/2}$ core-hole binding energies, respectively. We then compare the O $KL_{23}L_{23}$ and Ag $M_5N_{45}N_{45}$ Auger lines with the calculated local O $2p^4$ and local Ag $4d^8$ DOS, respectively, using the cluster method mentioned above. The values for the one-particle and two-particle model parameters used are listed in Table III. For the Racah *B* and *C* parameters, as well as for Slater F^2 integral, we have used Moore's free ion optical values,[31] since screening in the solid state occurs primarily for the monopole part (Racah *A*, Slater F^0) of the Coulomb interaction.[32]

We have split up the DOS's into a singlet and a triplet contribution. Because the O $KL_{23}L_{23}$ Auger transition for the ^3P states in atomic oxygen is forbidden and the Cu $L_{23}M_{45}M_{45}$ Auger matrix element for ^1G states in Cu metal is by far the largest,[33] we expect that the Auger transition matrix elements for singlets are larger than for triplets. The good resemblance of the Auger line shapes and the singlet two-hole DOS's indicates that this is indeed the case. The main peak in the spectra arises mainly from the multiplet split two-hole O 2*p*-2*p* and Ag 4*d*-4*d* states located around $2\varepsilon_p + U_{pp}(^1D) = 13.8$ eV

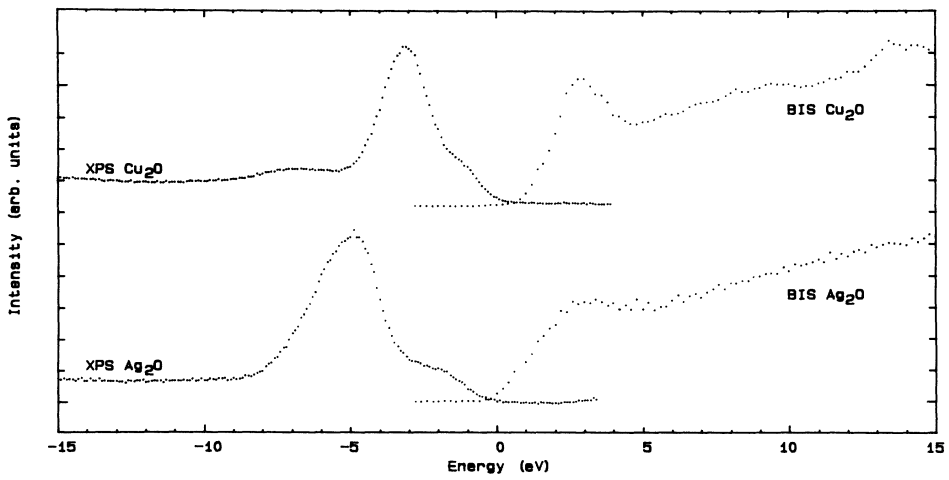

FIG. 6. Valence-band XPS (left) and conduction band BIS (right) from Cu_2O (top) and Ag_2O (bottom). The vertical scales of the different curves are independent.

and $2\varepsilon_d + U_{dd}(^1G) = 15.6$ eV, respectively, with $U_{pp}(^1D) = F^0 + F^2/25$ and $U_{dd}(^1G) = A + 4B + 2C$. These states hybridize with states having one hole on oxygen and another on silver, whose energies are $\varepsilon_p + \varepsilon_d = 8.3$ eV. The latter states in turn are strongly mixed with states having two holes located on different oxygen atoms or two holes on different silver atoms, with energies $2\varepsilon_p = 6.8$ eV and $2\varepsilon_d = 9.8$ eV, respectively. The result is a broad satellite structure ranging from 5 to 11 eV.

V. DISCUSSION

The close resemblance of the valence-band photoemission spectra and the calculated one-particle DOS's as well as that of the Auger-electron spectra and the calculated two-particle DOS's suggest that Ag_2O is indeed an essentially full band system.

Comparison of the valence-band spectra to recent band-structure calculations in the local-density approximation (LDA) by Czyzyk *et al.*[20] reveals some

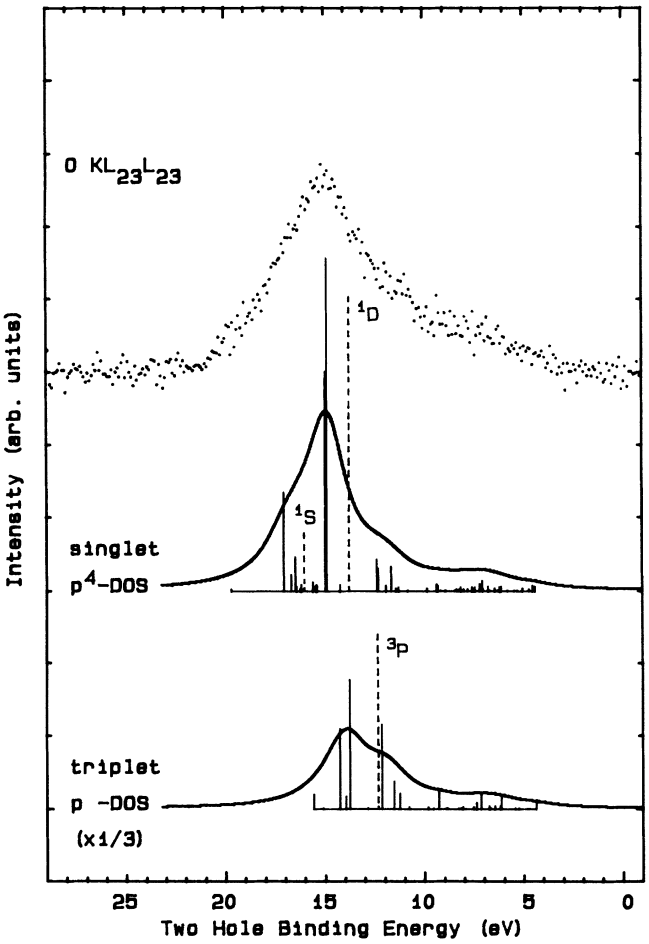

FIG. 7. O $KL_{23}L_{23}$ Auger spectrum and O $2p^4$ DOS from Ag_2O. The dotted line shows the experimental O $KL_{23}L_{23}$ Auger spectrum, for which the kinetic energy scale has been transformed into a two-hole binding energy scale by subtracting the O 1*s* binding energy. The spectrum has been corrected for analyzer transmission and electron scattering. The top solid line shows the singlet contribution to the O $2p^4$ DOS and the bottom solid line the triplet contribution (reduced by a factor 3), as calculated using a $(Ag_4O_5)^{6-}$ cluster with an O atom in the center and with parameters listed in Table III. A Lorentzian broadening of 2.4 eV has been applied. Also shown are the unbroadened states contributing to the DOS's (solid lines) and the multiplet split atomic states (dashed lines).

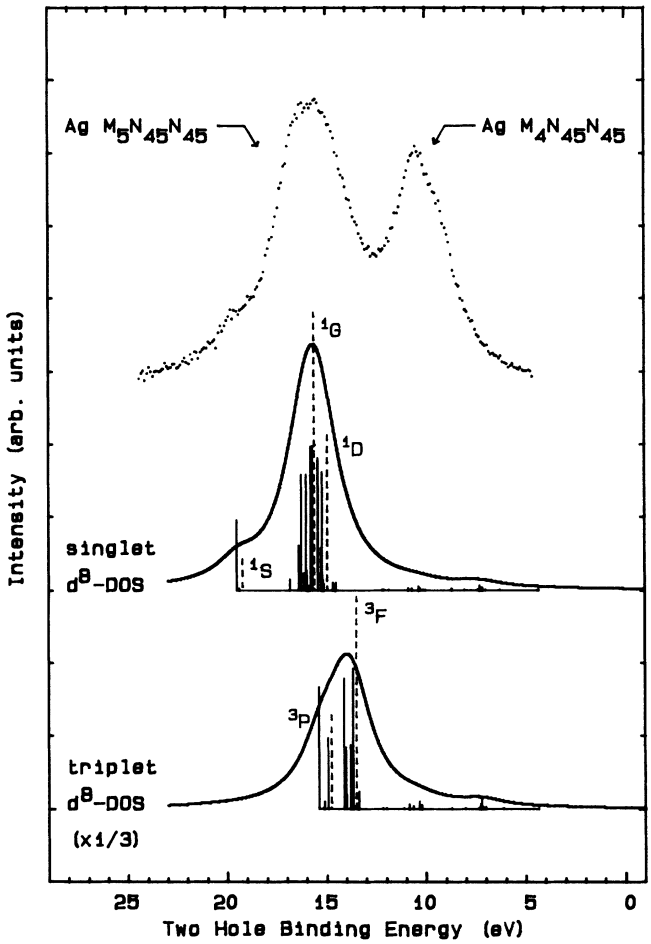

FIG. 8. Ag $M_5N_{45}N_{45}$, $M_4N_{45}N_{45}$ Auger spectrum and Ag $4d^8$ DOS from Ag_2O. The dotted line shows the experimental Ag $M_5N_{45}N_{45}$, $M_4N_{45}N_{45}$ Auger spectrum, for which the kinetic energy scale has been transformed into a two-hole binding energy scale for the $M_5N_{45}N_{45}$ by subtracting the Ag $3d_{5/2}$ binding energy. The spectrum has been corrected for analyzer transmission and electron scattering. The top solid line shows the singlet contribution to the Ag $4d^8$ DOS and the bottom solid line the triplet contribution (reduced by a factor 3), as calculated using a $(Ag_7O_2)^{3+}$ cluster with a Ag atom in the center and with parameters listed in Table III. A Lorentzian broadening of 2.4 eV has been applied. Also shown are the unbroadened states contributing to the DOS's (solid lines) and the multiplet split atomic states (dashed lines).

differences, see Fig. 3. First of all, the theoretical curves have been shifted by 1.8 eV to higher binding energy to align the main peak. More important, however, is that the structure is quite different especially on the high-energy side, which is probably a result of an incorrect value for $\varepsilon_p-\varepsilon_d$. Doing the same Slater Koster LCAO-TB fit to these calculations as have been done to the measured spectra above, we obtain values for $\varepsilon_p-\varepsilon_d$ which are about 2 eV larger (i.e., less negative) than shown in Table III. The same problem has also been encountered for Cu_2O, where the band-structure calculations[1] give about 1.5 eV larger (i.e., more positive) values for $\varepsilon_p-\varepsilon_d$ than listed in Table III. This discrepancy is fairly common in band-structure calculations of transition-metal compounds as discussed by van der Laan *et al.*[34]

The oxygen-to-metal d transfer integrals in Ag_2O are smaller than in Cu_2O (Table III). The difference is about 30% for $(pd\sigma)$. Following Harrison's relationship[24] that the transfer integral is proportional to $r^{3/2}/D^{7/2}$, where r is the d orbital radius and D the anion-cation distance (Table I), a reduction of about 5% is calculated. Although indicating the right trend, this value is still too small.

The on-site $d-d$ Coulomb interaction in Ag_2O [$U_{dd}(^1G)=5.8$ eV] is smaller than in Cu_2O [$U_{dd}(^1G)=9.2$ eV], as can be expected from the fact that the Ag 4d wave function has a larger radial extent than that of the Cu 3d. In the metallic case, the d-d Coulomb energies are smaller but show the same trend: 4.5 eV for Ag and 7.1 for Cu (Ref. 35). This can be understood by realizing that screening in metals is more effective. In Table V, we have listed the solid-state screening energies, calculated as the difference between the free ion d-d Coulomb values[31] and the observed solid-state values.

The on-site oxygen p-p Coulomb interaction in Ag_2O [$U_{pp}(^1D)=7.0$ eV] however, is larger than in Cu_2O [$U_{pp}(^1D)=5.7$ eV]. This is probably caused by differences in the screening energy, which would be about 4.4 eV in Ag_2O and 5.7 eV in Cu_2O, for an oxygen p-p free ion Coulomb energy of 11.4 eV,[36] as listed in Table V. A rough estimate of the change in screening can be made as follows. The screening due to polarizable ions varies as $\Sigma_{NN,NNN}\alpha R^{-4}$, where α is the ionic polarizability, R denotes the interatomic distance, and the sum is made over the nearest-neighbor (NN) (Ag or Cu) and next-nearest-neighbor (NNN) (O) atoms. Using $\alpha=1.6$, 2.4, and 3.2 Å^3 for Cu^+, Ag^+ and O^{2-}, respectively[37] and distances as given in Table I, we arrive at a screening contribution for Ag_2O which would be about 7% (=0.4 eV) smaller than for Cu_2O.

TABLE V. Two hole d-d (^1G) and p-p (^1D) Coulomb and screening energies (eV) in Ag_2O, Cu_2O, Ag, and Cu. The free ion Coulomb energies $U_{dd}(^1G)$ and $U_{pp}(^1D)$ are obtained from Refs. 31 and 36, respectively. The experimental Coulomb energies $U_{dd}(^1G)$ and $U_{pp}(^1D)$ in Ag_2O and Cu_2O are calculated from Table III, using $A+4B+2C$ and $F^0+F^2/25$, respectively. For Ag and Cu, the Coulomb energies are calculated using E_b(Ag $3d_{5/2}$)$-E_k$(Ag $M_5N_{45}N_{45}$)$-2E_b$(Ag d-band centroid) and E_b(Cu $2p_{3/2}$)$-E_k$(Cu $L_3M_{45}M_{45}$)$-2E_b$(Cu d-band centroid) (Ref. 35), respectively, which are slightly larger than $U_{dd}(^1G)$ according to the Cini-Sawatzky theory (Refs. 38 and 39).

	Ag_2O	Cu_2O	Ag	Cu
$U_{dd}(^1G)$ (free ion)	14.8	18.6	14.8	18.6
$U_{dd}(^1G)$ (expt)	5.8	9.2	4.5	7.1
Screening	9.0	9.4	10.3	11.5
$U_{pp}(^1D)$ (free ion)	11.4	11.4		
$U_{pp}(^1D)$ (expt)	7.0	5.7		
Screening	4.4	5.7		

More evidence that the Ag 4d shell is closed can be found from resonant photoemission and BIS, along with a comparison to Cu_2O. In the valence-band photoemission spectra, only a very weak resonance can be observed at 16.5 eV binding energy when scanning the photon energy through the Ag 4p edge ($h\nu\approx 56$ eV) as shown in Fig. 5. This is in contrast to Cu_2O, where a relatively strong resonance occurs at the Cu 3p edge ($h\nu=75.5$ eV).[40] Formally, a closed d shell should not show resonance structure. However, the d^{10} configuration mixes somewhat with higher energy $d^9(sp)^1$ states, where (sp) denotes the empty Cu 4s,4p or Ag 5s,5p states. This results in photoemission final states of $d^8(sp)^1$-like character at an energy given by $\varepsilon_d+U_{dd}(\Gamma)+\Delta_{dsp}$. Here Γ denotes a two-hole irreducible representation and Δ_{dsp} is the d-(sp) charge-transfer energy given by the energy distance between the d on-site energy ε_d and the bottom of the (sp) conduction band and is listed in Table IV. These final $d^8(sp)^1$ states can also be thought of as $d\rightarrow(sp)$ electron-hole excitations from a d^9 state. Using values from Tables III, IV, and V, we obtain a calculated onset for the "satellite" binding energy of 15.9 eV. The experimental onset in Ag_2O is at about 15.7 eV; slightly lower than the peak position of 16.5 eV. The intensity of this satellite peak far away from resonance is roughly proportional to the amount of $d^9(sp)^1$ character in the ground state, which in turn is inversely proportional to Δ_{dsp} and proportional to the d^{10}-$d^9(sp)^1$ hybridization transfer integral. Both the larger value of Δ_{dsp} in Ag_2O (5.2 eV) as compared to that in Cu_2O (4.7 eV) and the apparently smaller hybridization transfer integral are the cause of the much weaker intensity in Ag_2O as compared to Cu_2O.

A peak at 3 eV can be seen in the Cu_2O BIS spectrum. Assuming that at high electron and photon energies the σ (O 2p)/σ(Cu 3d) cross-section ratios in BIS and XPS are similar, this peak was attributed to empty states having Cu 3d character.[1] For Ag_2O, however, such a peak is not present or is very weak. This is consistent with the above reasoning about the expected $d^9(sp)^1$ character in the ground state of Cu_2O and Ag_2O. Recent x-ray-absorption spectroscopy measurements on Ag_2O at the Ag $L_{2,3}$ edge[20] (probing the empty d states), also show a much smaller peak than has been found for the Cu $L_{2,3}$ edge in Cu_2O (Ref. 41).

VI. RELEVANCE TO HIGH-T_c SUPERCONDUCTIVITY

Some of the important facts, which are believed to be of basic importance for an understanding of high-T_c su-

perconductivity, and which are obtained from detailed spectroscopic studies of Cu_2O and CuO are[1,2] outlined as follows.

The Cu $3d$ ionization states in Cu_2O are closer to the Fermi level than the O $2p$ states so that upon adding holes as one does in going from Cu_2O to CuO, the holes are expected to appear first in the Cu $3d$ states.

The Cu d-d Coulomb interaction is large ($U \approx 8.2$ eV) and larger than the O $2p$–Cu $3d$ charge-transfer energy ($\Delta \approx 2.75$ eV) in CuO, leading to a charge-transfer insulator and to localized moments on the Cu.

The O $2p$–Cu $3d$ hybridization is very strong leading to very large antiferromagnetic superexchange interactions in CuO and the high T_c's.

The first ionization states in CuO are of primarily O $2p$ character according to the phase diagram of Zaanen *et al.*[42] with $U > \Delta$, and so, upon further oxidation or substitution, the holes will be in the O $2p$ band.

The exchange interaction between the O $2p$ holes and the Cu $3d$ spins is extremely large which can lead to local singlet formation.[43–46]

In this respect, it is interesting to note that $\varepsilon_p - \varepsilon_d$ is -1.5 eV in Ag_2O, whereas it has the opposite sign in Cu_2O and is $+2.5$ eV. Comparing this value for Cu_2O to the O $2p$ to Cu $3d$ charge-transfer energy (Δ) of 2.75 eV for CuO (Ref. 40), we can expect that Δ is negative in AgO and of the order of -1–-2 eV. This implies that the ground-state configuration of AgO would, if the crystal structure were the same, consist of a hole mainly in the oxygen band and a full Ag $4d$ band (Ag^+), contrary to that of CuO. Also, if it were possible to replace Cu by Ag in the CuO_2 planes in the insulating high-T_c compounds, then this would probably result in replacing Cu^{2+} by Ag^+ together with hole doping in the oxygen band, rather than by Ag^{2+}.

Upon further oxidation or hole doping of AgO, provided this is possible, the interesting question arises whether or not a localized hole can be formed at the Ag site. Equivalently, it would be interesting to determine the character of the first ionization states and the type of the insulating gap of AgO. At first sight, it is tempting to use the phase diagram of Zaanen *et al.*,[42] but now with the oxygen taking over the role of the cation and the silver that of the anion, U is here the on-site oxygen p-p Coulomb interaction, which will have a somewhat smaller value than 5.8 eV as in Ag_2O due to the larger coordination number, and Δ is the negative of $\varepsilon_p - \varepsilon_d$, which is about 1.5 eV. This will then give a Ag $4d$-like first ionization state and a charge-transfer-like insulating gap, where the first affinity states are O $2p$-like. However, the oxygen bandwidth w will be around 4–5 eV, due to direct oxygen-oxygen overlap as in CuO. So, the Anderson impurity approach as used by Zaanen *et al.* is no longer applicable. Instead one has to deal with an Anderson lattice problem, for which, up to now, no solution is known.

VII. STABILITY OF NOBLE-METAL COMPOUNDS

In Table VI, we have listed the energy positions of the d-band centroid (ε_d) relative to the Fermi level and the work functions of the Cu, Ag, and Au metal, thereby suggesting that their sum can be used as a measure of the energy cost of the reaction $Cu^+ \rightarrow Cu^{2+} + e^-$, $Ag^+ \rightarrow Ag^{2+} + e^-$, and $Au^+ \rightarrow Au^{2+} + e^-$, respectively, where e^- denotes a free electron. This energy cost (7.7, 9.8, and 8.9 eV, respectively) has to be met by the reduction reaction of the oxidator. Therefore, dihalides and chalcogenides of copper are more stable than those of silver and gold.

TABLE VI. Work functions, d-band centroids relative to the Fermi level, and two-hole d-d(^1G) Coulomb energies (eV) of Cu, Ag, and Au. The work functions are obtained from Refs. 47 and 48. For Au, the centroid of the $d_{5/2}$ band has been taken.

	Cu	Ag	Au
Work function	4.6	4.3	5.1
d-band centroid (ε_d)	3.1	5.5	3.8
$U_{dd}(^1G)$	7.1	4.5	≈ 2

AgO has the interesting property that no magnetic ordering could be observed using neutron diffraction, even down to liquid-helium temperatures,[4] in contrast to the antiferromagnetic CuO. The crystal structure of AgO is also different from CuO. AgO crystallizes in a monoclinic[4,17,49] or tetragonal[5] structure. In both structures there are two nonequivalent Ag sites: Ag(I) is linearly coordinated by two oxygens with a Ag-O distance of 2.18 Å and Ag(III) is almost square planar coordinated by four oxygens with a Ag-O distance of 2.03 Å. In CuO, which has a monoclinic crystal structure, all Cu are surrounded by O at a distance of 1.95 Å in an almost square planar coordination.[6] The existence of Ag^+ and low-spin Ag^{3+} in AgO has been proposed to explain the diamagnetic behavior of AgO as well as the two coordinations. Apparently the change in Madelung potential as well as the ligand field hybridization in the altered crystal structure of AgO are sufficient to overcome $U_{dd}(^1G) = 5.8$ eV, which is the energy required to go from a twice Ag^{2+} configuration to a Ag^+ and Ag^{3+} configuration. These changes however, are not sufficient for CuO where $U_{dd}(^1G)$ is 8.2 eV. It is interesting to note that in Au compounds U_{dd} is even smaller, making the existence of mixed Au^+ and Au^{3+} rather than twice Au^{2+} in Au compounds quite common.

From Table VI, the sum of the work function, the d-band centroid energy position (ε_d) and U_{dd} can be calculated, which can be considered as the energy required for the reaction $Cu^{2+} \rightarrow Cu^{3+} + e^-$, $Ag^{2+} \rightarrow Ag^{3+} + e^-$, and $Au^{2+} \rightarrow Au^{3+} + e^-$. For Cu and Ag, we find values of 14.8 and 14.3 eV, respectively, which prevent Cu or Ag trihalides to exist. The stability of Au trihalides, on the other hand, can be understood as this sum is only ≈ 11 eV, which can be even more reduced by the extra ligand hybridization stabilization and Madelung potential mentioned above.

VIII. CONCLUSIONS

Ag_2O is an essentially full band system, the valence-band electronic structure of which can be described using

a one-particle band theory. The *p-d* transfer integral in Ag_2O [$(pd\sigma)=1.3$ eV, $(pd\pi)=0.6$ eV] is less than in Cu_2O, consistent with the larger interatomic distances in Ag_2O. In contrast to Cu_2O, the on-site energy for the *d* orbital ($\varepsilon_d=4.9$ eV) is higher (farther from the Fermi level) than for the *p* orbital ($\varepsilon_p=3.4$ eV) in Ag_2O.

The O $KL_{23}L_{23}$ and Ag $M_5N_{45}N_{45}$ Auger-electron structures can be described within a two-particle cluster theory. The on-site *d-d* Coulomb and exchange energy in Ag_2O [$U_{dd}(^1G)=5.8$ eV] is smaller than in Cu_2O, as the Ag *d* orbital is spatially more extended. The on-site oxygen *p-p* correlation energy in Ag_2O [$U_{pp}(^1D)=7.0$ eV] is larger than in Cu_2O, as screening in Ag_2O is less effective, mainly due to larger interatomic distances.

From the comparison of $\varepsilon_p-\varepsilon_d$ in Ag_2O and Cu_2O, we would expect the holes to be in the oxygen band in AgO for the same crystal structure as CuO, while we expect and see the holes in the Cu 3*d* states in CuO. Apparently, however, a change in the crystal structure of AgO is sufficient to stabilize the charge disproportionated Ag^+ and Ag^{3+} states, as well as to prevent strong local moments at the Ag sites, unlike in CuO. Upon doping of AgO, however, it depends on the magnitude of the oxygen bandwidth relative to the on-site oxygen *p-p* Coulomb interaction, whether or not a localized hole can be formed at the Ag site, making AgO an interesting material for further study.

ACKNOWLEDGMENTS

This work was supported by the Netherlands Foundation for Fundamental Research on Matter (FOM), the Netherlands Foundation for Chemical Research (Stichting Scheikundig Onderzoek in Nederland), the Netherlands Organization for the Advancement of Pure Research (NWO) and the German Ministry for Research and Technology [Bundesministerium fur Forschung und Technologie, (Germany), Project No. 05 390CAB].

*Present address: Laboratory for Electron Spectroscopy, 61 rue de Bruxelles, B-5000 Namur, Belgium.

†Present address: 2nd Institut of Experimental Physics, University of Hamburg, Luruper Ch. 149, D-2000 Hamburg 50, Federal Republic of Germany.

[1]J. Ghijsen, L. H. Tjeng, J. van Elp, H. Eskes, J. Westerink, G. A. Sawatzky, and M. T. Czyzyk, Phys. Rev. B **38**, 11 322 (1988).

[2]L. H. Tjeng, J. van Elp, P. Kuiper, and G. A. Sawatzky (unpublished); H. Eskes, L. H. Tjeng, and G. A. Sawatzky, Phys. Rev. B (to be published).

[3]A. F. Wells, *Structural Inorganic Chemistry,* 5th ed. (Clarendon, Oxford, 1984), p. 1120.

[4]V. Scatturin, P. L. Bellon, and A. J. Salkind, J. Electrochem. Soc. **108**, 819 (1961).

[5]K. Yvon, A. Bezinge, P. Tissot, and P. Fisher, J. Solid State Chem. **65**, 225 (1986).

[6]S. Åsbrink and L. J. Norrby, Acta Crystallogr. Sect. B **26**, 8 (1970).

[7]K. C. Prince, G. Paolucci, and A. M. Bradshaw, Surf. Sci. **175**, 101 (1986).

[8]R. B. Grant and R. M. Lambert, Surf. Sci. **146**, 256 (1984).

[9]W. Segeth, J. H. Wijngaard, and G. A. Sawatzky, Surf. Sci. **194**, 615 (1988).

[10]B. V. Tilak, R. S. Perkins, H. A. Kozlowska, and B. E. Conway, Electrochim. Acta **17**, 1447 (1972).

[11]A. Kunugi, S. Miyoshi, and S. Nagaura, Bull. Chem. Soc. Jpn. **51**, 700 (1978).

[12]M. A. Barteau and R. J. Madix, in *The Chemical Physics of Solid Surfaces and Heterogeneous Catalysis,* edited by D. A. King and D. P. Woodruff (North-Holland, Amsterdam, 1982), Vol. 3, Chap. 4.

[13]R. A. van Santen and H. P. C. E. Kuipers, Adv. Catal. **35**, 265 (1987).

[14]E. L. Evans, J. M. Thomas, M. Barber, and R. J. M. Griffiths, Surf. Sci. **38**, 245 (1973).

[15]T. Dickinson, A. F. Povey, and P. M. A. Sherwood, J. Solid State Chem. **13**, 237 (1975).

[16]J. S. Hammond, S. W. Gaarenstroom, and N. Winograd, Anal. Chem. **47**, 2193 (1975).

[17]G. Schön, Acta Chem. Scand. **27**, 2623 (1973).

[18]S. W. Gaarenstroom and N. Winograd, J. Chem. Phys. **67**, 3500 (1977).

[19]C. D. Wagner, Anal. Chem. **44**, 967 (1972).

[20]Very recently, an x-ray-absorption study combined with *ab initio* band-structure calculations has been carried out by M. T. Czyzyk, R. A. de Groot, G. Dalba, P. Fornasini, A. Kisiel, F. Rocca, and E. Burattini, Phys. Rev. B **39**, 9831 (1989).

[21]J. C. Slater and G. F. Koster, Phys. Rev. **94**, 1498 (1954).

[22]J. S. Griffith, *The Theory of Transition Metal Ions* (Cambridge University Press, Cambridge, 1961).

[23]J. C. Slater, *Quantum Theory of Atomic Structure* (McGraw-Hill, New York, 1960), Vols. 1 and 2.

[24]W. A. Harrison, *Electronic Structure and the Properties of Solids* (Freeman, San Francisco, 1980).

[25]G. V. Samsonov, *The Oxide Handbook* (Plenum, New York, 1973).

[26]P. G. Dickens, R. Heckingbottom, and J. W. Linnett, Trans. Faraday Soc. **65**, 2235 (1969).

[27]J. J. Yeh and I. Lindau, At. Data Nucl. Data Tables **32**, 1 (1985).

[28]M. Prutton, *Surface Physics,* 2nd ed. (Oxford University Press, Oxford, 1983), p. 23.

[29]E. Fortin and F. L. Weichman, Phys. Status Solidi A **5**, 515 (1964).

[30]E. Tselepis and E. Fortin, J. Mater. Sci. **21**, 985 (1986).

[31]C. E. Moore, *Atomic Energy Levels,* Natl. Bur. Stand. (U.S.) Circ. No. 467 (U.S. GPO, Washington D.C., 1958), Vols. 1–3.

[32]D. van der Marel and G. A. Sawatzky, Phys. Rev. B **37**, 10 674 (1988).

[33]E. Antonides, E. C. Janse, and G. A. Sawatzky, Phys. Rev. B **15**, 1669 (1977).

[34]G. van der Laan, G. A. Sawatzky, C. Haas, and H. W. Myron, Phys. Rev. B **20**, 4287 (1979).

[35]J. C. Fuggle, P. Bennett, F. U. Hillebrecht, A. Lenselink, and G. A. Sawatzky, Phys. Rev. Lett. **24**, 1787 (1982).

[36]J. E. Huheey, *Inorganic Chemistry,* 3rd ed. (Harper and Row, New York, 1983), pp. 42–48, and references therein.

[37]J. Tessman, A. Kahn, and W. Schockley, Phys. Rev. **92**, 890 (1953).

[38]M. Cini, Solid State Commun. **24**, 681 (1977); Phys. Rev. B **17**, 2788 (1978).

[39]G. A. Sawatzky, Phys. Rev. Lett. **34**, 504 (1977).
[40]M. R. Thuler, R. L. Benbow, and Z. Hurych, Phys. Rev. B **26**, 669 (1982).
[41]M. Grioni, J. B. Goedkoop, R. Schoorl, F. M. F. de Groot, J. C. Fuggle, F. Schäfers, E. E. Koch, G. Rossi, J.-M. Esteva, and R. C. Karnatak, Phys. Rev. B **39**, 1541 (1989); M. Grioni, M. T. Czyzyk, F. M. F. de Groot, J. C. Fuggle, and B. E. Watts, *ibid.* **39**, 4886 (1989).
[42]J. Zaanen, G. A. Sawatzky, and J. W. Allen, Phys. Rev. Lett. **55**, 418 (1985).
[43]F. C. Zhang and T. M. Rice, Phys. Rev. B **37**, 3759 (1988).
[44]H. Eskes and G. A. Sawatzky, Phys. Rev. Lett. **61**, 1415 (1988).
[45]A. K. McMahan, R. M. Martin, and S. Satpathy, Phys. Rev. B **38**, 6650 (1988).
[46]E. B. Stechel and D. R. Jennison, Phys. Rev. B **40**, 6919 (1989).
[47]A. W. Dweydari and C. H. B. Mee, Phys. Status Solidi A **27**, 223 (1975).
[48]D. E. Eastman, Phys. Rev. B **32**, 1 (1970).
[49]R. Holm and S. Storp, Appl. Phys. **9**, 217 (1976).